scientific reports

Check for updates

OPEN

Research on the contact characteristics of rocker arm gears in shearer under lubrication containing coal powder impurities

Xin Wang, Rennan Wu✉, Libin Wang & Yangxi Bai

To study the contact characteristics of the shearer rocker arm gear transmission system under lubrication containing coal powder impurities, the MG500/1130 shearer rocker arm transmission system was selected as the research object, and a gear elastohydrodynamic lubrication (EHL) model was constructed based on Hertz–Reynolds theory. Considering the impact of coal powder impurities on the viscosity of the lubricant, the kinematic viscosity of coal powder-laden lubricant was measured under different coal powder particle sizes, concentration ratios, and temperatures using a mixed orthogonal experimental method. A polynomial fitting method was employed to establish the functional relationship between particle size, concentration ratio, temperature, and viscosity of the lubricant. A multi-software collaborative simulation approach was used to construct a simulation model of the shearer rocker arm gear transmission system, analyzing the effects of coal powder-laden lubricant with different particle sizes and concentration ratios on gear contact stress and lubricant film thickness. The results indicate that, under four different conditions of coal powder particle size and concentration, the maximum contact stress of the Z1 gear in the rocker arm transmission system ranged from 1134 to 1177 MPa. As the particle size and concentration of coal powder increased, the maximum contact stress of the Z1 gear showed a decreasing trend. Additionally, under the same coal powder particle size and concentration, the contact stress of the gears near the output end was significantly higher than that of the gears near the input end. The minimum lubricant film thickness during gear meshing under the four conditions varied between 0.08 μm and 0.26 μm. Furthermore, the coal powder particle size and concentration in the lubricant were positively correlated with the lubricant film thickness: larger particle sizes and higher concentrations resulted in greater minimum lubricant film thickness. These findings provide theoretical support for improving the reliability of the shearer rocker arm transmission system.

Keywords Shearer rocker arm, Gear transmission system, Impurity-containing lubrication, Kinematic viscosity, Contact characteristics

The gear transmission system of the shearer rocker arm is a critical component for transmitting the drum's torque, and its performance directly affects the shearer's operational efficiency and reliability. The issue of contact stress during gear meshing has received considerable attention, and numerous scholars, both domestically and internationally, have studied this.

In theoretical research on gear contact stress, Zhonghua Lü[1] derived a formula to calculate the contact stress at any contact point on the tooth surface along the meshing line using Hertzian contact theory and obtained the distribution characteristics of contact stress along the meshing line under different parameters through MATLAB. Yuda Wang et al.[2] considered load distribution between teeth and applied Hertzian principles to perform a contact analysis on the tooth surface. The results were consistent with finite element simulations and experimental findings. Jianjun Feng et al.[3] calculated the maximum contact stress of profile-shifted involute cylindrical gears based on Hertzian formulas. Long Xiang et al.[4] proposed a method for calculating tooth surface contact stress using a combined Hertz–Winkler model. Using this method, they determined the maximum contact stress and its variation under different loads and meshing positions, comparing it with results from finite element analysis. Guoyun Li et al.[5] utilized cylindrical contact mechanics principles and simulated gear contact

School of Mechanical Engineering, Liaoning Technical University, Fuxin 123000, China. ✉email: 1910507133@qq.com

stress using the Ansys/LS-DYNA platform, comparing the simulation results with Hertzian theory and achieving close agreement. Su Yang[6] calculated working stress on the tooth surface using three methods: empirical, theoretical, and numerical, identifying the location of the maximum contact stress. Ganhua Liu et al.[7] derived the helical gear tooth surface contact stress based on Hertzian principles and, through dynamic simulation analysis, obtained the dynamic contact stress during the meshing process. Zhimin Fan et al.[8] developed a fractal contact model for gears based on fractal and Hertzian theories, taking influencing factors into account, with results indicating the model's effectiveness for double-involute gear contact stress. Xiangmao Huang[9] developed a mathematical model for contact stress in cycloidal gears along the tooth width direction by combining force balance and deformation coordination equations, and then performed the calculations.

In experimental studies on gear lubrication, Peter[10] analyzed the contact stress between gear teeth using reflective photoelasticity, comparing experimentally assessed contact stress with analytically computed values and employing Airy's stress function or Hertzian relationships. Xiaopeng Yang et al.[11] analyzed helical gear contact stress through finite element simulations and experimental validation, examining the impact of friction coefficient on contact stress for a given friction coefficient. Shenghui Wang et al.[12] proposed an optimization model with a simplified algorithm of the loaded tooth contact analysis with errors (ELTCA) for modified helical face gears, and it can programmatically optimize the contact stress with edge contact avoidance. Long Chen et al.[13] developed a multi-piece stitched NURBS surface parametric model for Isogeometric Analysis (IGA), deriving the calculation formula and comparing the results with Hertzian contact analysis outcomes under frictionless conditions.

In simulation-based studies of gear contact and transmission, Yu Zhu et al.[14] conducted a study on the MG500/1180 shearer model, analyzing the strength and lifespan of various components within its transmission system. Hongbo Cui[15] modeled involute cylindrical spur gears by combining MATLAB and SolidWorks and conducted a simulation analysis of their contact characteristics. Aimin Liu et al.[16] performed finite element analysis (FEA) on the tooth surface contact stress, comparing the simulation results with the calculated values from Hertzian formulas. Feng Yang et al.[17] performed a simulation analysis of the contact stress in reducer gears, considering two types of assembly errors in their analysis. Guoping Yan et al.[18] derived a new involute equation using standard involute equations combined with the Walker modification method. Gear modeling was performed using APDL based on the new involute equation, and dynamic simulations were conducted according to contact principles. Yangang Wei et al.[19] conducted a comprehensive finite element analysis of contact stress during the meshing process of involute spur gears and compared the results with Hertzian formula calculations. Guifan Zhao et al.[20] constructed a gear model in ANSYS based on the mathematical model of gear tooth profile and solved for contact stress using the full Newton–Raphson method according to the meshing process, with ANSYS results closely matching empirical findings. Jia Li et al.[21] used CAD technology to build a gear model, performing simulation analysis in ANSYS and comparing the results with theoretical verification.

It is worth noting that most of the aforementioned studies are based on ideal lubrication conditions and overlook the presence of coal powder particles, which are commonly found in underground coal mine environments. As solid particles in the lubrication system, coal powder particles can significantly alter the lubrication regime, affect the contact pattern and stress distribution on gear meshing surfaces, and consequently impact the operational efficiency and lifespan of the entire transmission system. However, systematic studies on the contact characteristics of gears under lubrication conditions contaminated with coal powder particles remain insufficient, especially in terms of modeling approaches and experimental validation.

In light of this, this paper focuses on the MG500/1130 shearer rocker arm transmission system, deeply exploring the variation of gear contact stress in a lubricating environment containing coal powder impurities. This research is not only significant for enhancing the reliability of shearers but also plays a crucial role in ensuring their operational efficiency, providing important engineering guidance.

Theoretical model of gear contact in the rocker arm transmission system

Main structure and parameters of the rocker arm transmission system

This study focuses on the MG500/1130 shearer transmission system, which consists of a two-stage helical gear reduction system and two single-stage planetary gear reduction systems. Referring to Fig. 1, which illustrates the transmission system, the gears in the gear set are named sequentially starting from the motor according to the transmission order: the first gear set consists of input gear 1 (Z_1), idler gear 1 (Z_2), and output gear 1 (Z_3);

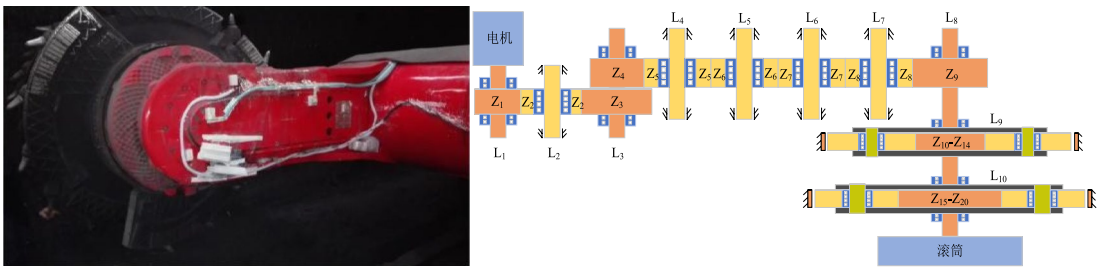

Fig. 1. Arm transmission system of the MG500/1130 shearer.

Gear	Z_1	Z_2	Z_3	Z_4	Z_5	Z_6	Z_7	Z_8	Z_9
Module(mm)	8	8	8	9	9	9	9	9	9
Number of teeth	29	39	39	27	37	36	37	38	37
Face width(mm)	80	80	80	98	98	98	98	98	98

Table 1. Structural parameters of helical gears.

Planet gear set number	Parameter	Sun gear (Z_{10},Z_{15})	Planet gear ($Z_{11}Z_{12}Z_{13}$,$Z_{16}Z_{17}Z_{18}Z_{19}$)	Epicyclic gear train (Z_{14},Z_{20})
1	Module(mm)	7	7	7
	Number of teeth	21	41	105
	Face width(mm)	100	85	87
2	Module(mm)	9	9	9
	Number of teeth	26	31	90
	Face width(mm)	195	185	172

Table 2. Structural parameters of planetary gear set.

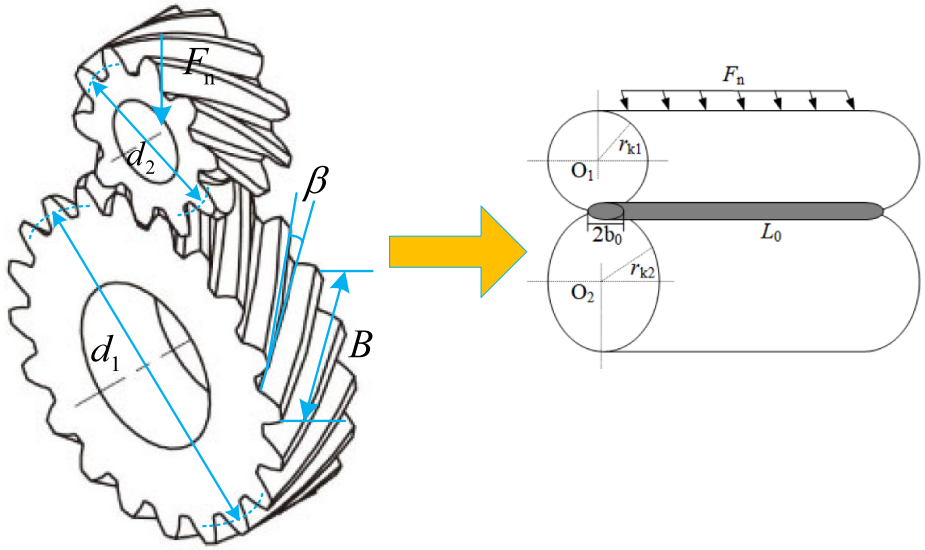

Fig. 2. Gear contact model.

the second gear set comprises input gear 2 (Z_4), idler gears 2 (Z_5, Z_6, Z_7, Z_8), and output gear 2 (Z_9); the first planetary gear set includes sun gear 1 (Z_{10}), planet gears 1 (Z_{11}, Z_{12}, Z_{13}), and epicyclic gear train 1 (Z_{14}); the second planetary gear set consists of sun gear 2 (Z_{15}), planet gears 2 (Z_{16}, Z_{17}, Z_{18}, Z_{19}), and epicyclic gear train 2 (Z_{20}). $L_1 \sim L_8$ represent gear shafts, while $L_9 \sim L_{10}$ denote the planetary carriers. The structural parameters of all the helical gears, as well as those of planetary gear sets 1 and 2, are detailed in Tables 1 and 2. The helix angle of all the above gears is 12°, and the parameters are based on the design manual of the MG500/1130 shearer.

Elastohydrodynamic lubrication model for gear contacts

The transmission system of the shearer cutting unit is a gear-driven system. When considering only elastic deformation at the gear contact interface, the Hertz contact theory can be applied. According to this theory, when any two bodies made of homogeneous and isotropic materials come into contact along a line or at a point under pressure, deformation and normal stress occur in the contact region. As shown in Fig. 2, when gears are engaged, the length of the contact region is much smaller than the gear width, allowing the contact to be approximated as that between two cylinders with radii defined by the contact curvature. When these two cylinders are subjected to an external load F_n, elastic deformation occurs in the contact area. The cross-section of the deformation appears elliptical, with a contact radius b_0, and the deformation extends along the contact line L_0 to form an elliptical cylinder.

The contact line length L_0 can be expressed as[22]:

$$L_0 = \frac{B}{Z_\varepsilon^2 \cos\beta_b} \tag{1}$$

$$Z_\varepsilon = \sqrt{\frac{4-\varepsilon_\alpha}{3}(1-\varepsilon_\beta)+\frac{\varepsilon_\beta}{\varepsilon_\alpha}} \tag{2}$$

In the equations, ε_α represents the overlap ratio of the helical gear,$\varepsilon_\alpha = \frac{z_1(\tan\alpha_{at1}-\tan\alpha_t)+z_2(\tan\alpha_{at2}-\tan\alpha_t)}{2\pi}$; subscripts 1 and 2 refer to the driving and driven gears, respectively; z_1, z_2 represent the number of teeth of the two gears,$\alpha_{at1} = arc\cos\frac{z_1\cos\alpha_t}{z_1+2h_a^*\cos\beta}$,$\alpha_{at2} = arc\cos\frac{z_2\cos\alpha_t}{z_2+2h_a^*\cos\beta}$;$\alpha_t$isthetransversepressureangle,$\alpha_t = \arctan\frac{\tan\alpha_n}{\cos\beta}$, and β is the helix angle. ε_β represents the axial overlap ratio of the helical gear,$\varepsilon_\beta = \frac{Bz_1\tan\beta}{d_1\pi}$; B is the tooth width, and d_1 is the pitch circle diameter of the driving gear.

The Hertzian contact stress can be expressed as[22]:

$$\sigma_H = \sqrt{\frac{F_n}{L_0 r_{k\sum}\pi\left[\frac{1-\mu_1^2}{E_1}+\frac{1-\mu_2^2}{E_2}\right]}} \tag{3}$$

In the equations, subscripts 1 and 2 represent the driving and driven gears, respectively; μ_1, μ_2 are the Poisson's ratios of the two gears, while E_1, E_2 are their elastic moduli. The equivalent radius of curvature is given by $r_{k\sum} = \frac{r_{k1}r_{k2}}{r_{k1}+r_{k2}} = \frac{d_1\sin\alpha_t}{2\cos\beta_b}\frac{u}{u+1}$, where r_{k1}, r_{k2} represent the curvature radii of the driving and driven gears at the meshing point, respectively. β_b represents the base helix angle, and i is the transmission ratio. The external load is defined as $F_n = 2K_0T_1/(d_1\cos\alpha_n\cos\beta)$, where K_0 is the load coefficient, T_1 is the torque of the driving gear, and α_n is the normal pressure angle.

The Hertzian contact radius b_0 can be expressed as[11]:

$$b_0 = \sqrt{\frac{4F_n}{\pi L_0}\left(\frac{1-\mu_1^2}{E_1}+\frac{1-\mu_2^2}{E_2}\right)\frac{r_{k1}r_{k2}}{r_{k1}+r_{k2}}} \tag{4}$$

The lubrication problem of gear contact in the rocker arm drive system can be considered as a line contact elastohydrodynamic problem, with a schematic diagram of the elastic deformation in the gear contact area shown in Fig. 3. The line contact elastohydrodynamic problem can be solved using Hertz contact theory and Reynolds lubrication theory, which include the following five fundamental equations:

1) Reynolds equation[23]:

$$\frac{d}{dx}\left(\frac{\rho h^3}{\eta}\frac{dp}{dx}\right) = 12u\frac{d(\rho h)}{dx} \tag{5}$$

In the equation, ρ represents the lubricant density, p represents the contact area pressure, u represents the entrainment velocity, and h represents the lubricant film thickness.

2) Film geometry equation[23]:

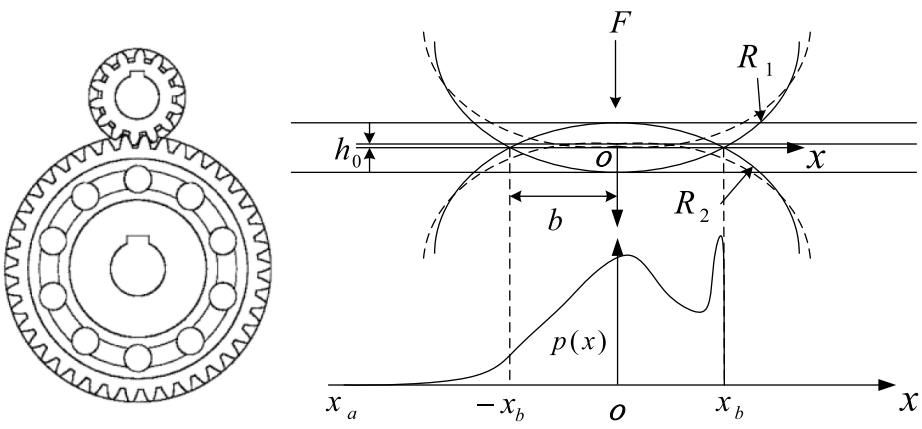

Fig. 3. Schematic diagram of elastic deformation in the gear contact area.

$$h(x) = h_0 + \frac{x^2}{2R^*} - \frac{2}{\pi E^*}\int_{-\infty}^{x} p(s)\ln(x-s)^2 ds \tag{6}$$

In the equation, h_0 represents the central lubricant film thickness, R^* represents the equivalent curvature radius and $R^* = \frac{R_1 R_2}{R_1+R_2}$, E^* represents the equivalent elastic modulus and $\frac{1}{E^*} = \frac{1-\nu_1^2}{E_1} + \frac{1-\nu_2^2}{E_2}$, E_1 and ν_1 represent the elastic modulus and Poisson's ratio of the driving gear, respectively; E_2 and ν_2 represent the elastic modulus and Poisson's ratio of the driven gear, respectively.

3) Lubricant viscosity-pressure equation[23]:

$$\eta = \eta_0(1+cp)^n \tag{7}$$

In the equation, η_0 represents the dynamic viscosity of the lubricant under standard atmospheric pressure, and c and n is a viscosity parameter that can be measured experimentally.

4) Lubricant density equation[23]:

$$\rho = \rho_0\left(1 + \frac{0.6\times10^{-9}p}{1+1.7\times10^{-9}p}\right) \tag{8}$$

5) Load balance equation[23]:

$$F = \int_{x_a}^{x_b} p dx \tag{9}$$

Let $H = \frac{hR^*}{b^2}$,$W = \frac{F}{E^*R^*}$,$U = \frac{\eta_0 u}{E^*R^*}$,$\overline{\eta} = \frac{\eta}{\eta_0}$,$\overline{\rho} = \frac{\rho}{\rho_0}$,$X = \frac{x}{b}$ and $P = \frac{p}{p_H}$,where b represents the half-width of the contact area and $b = \sqrt{\frac{8}{\pi}\frac{FR^*}{E^*}}$, p_H is the maximum contact pressure and $p_H = \frac{E^*b}{4R^*}$. By nondimensionalizing Eqs. (5) to (9), the following expression is obtained:

$$\begin{cases} \frac{d}{dX}\left(\frac{\overline{\rho}H^3}{\overline{\eta}}\frac{dP}{dX}\right) = \frac{3}{4}\frac{\pi^2 U}{W^2}\frac{d(\overline{\rho}H)}{dX} \\ H = H_0 + \frac{4W}{\pi}X^2 - \frac{4}{\pi}\sqrt{\frac{2W}{\pi}}\int_{X_b}^{X_a} P(S)\ln(X-S)^2 dS \\ \overline{\eta} = (1+cPp_H)^n \\ \overline{\rho} = \left(1 + \frac{0.6\times10^{-9}Pp_H}{1+1.7\times10^{-9}Pp_H}\right) \\ \int_{X_a}^{X_b} P dX = \frac{\pi}{2} \end{cases} \tag{10}$$

Due to the highly nonlinear integral equation in formula (10), which has no analytical solution, numerical differentiation is typically used for computation. The calculation process is shown in Fig. 4.

Experiment on the kinematic viscosity of coal powder-laden lubricants

Lubricants plays a crucial role in mechanical operation by reducing friction, cleaning, and dissipating heat. Among its various properties, kinematic viscosity is a key performance indicator, as it directly influences the oil film thickness and lubrication effectiveness. A higher kinematic viscosity enables the formation of a thicker oil film, thereby improving lubrication performance; however, it reduces fluidity and limits heat dissipation. Conversely, lower viscosity enhances fluidity and cooling efficiency, but provides insufficient lubrication protection. Therefore, it is essential to select an appropriate viscosity grade based on the operating conditions of the equipment.

The gear transmission system of the cutting arm in shearers typically uses medium extreme pressure industrial gear lubricant N320, whose main technical parameters are listed in Table 3. This lubricant exhibits excellent extreme-pressure and anti-wear properties, forming a stable oil film under high loads and extreme conditions to reduce gear surface wear and extend equipment lifespan. N320 also offers good thermal oxidation stability, heat transfer capability, and resistance to deposit formation, which effectively suppresses sludge generation, keeps the system clean, and ensures long-term stable operation of the equipment.

The contact model of the rocker arm drive system indicates that the viscosity of the lubricant between the gears significantly affects the contact stress. In conditions of high dust and strong vibration underground, the rocker arm lubrication system can mix in a certain amount of coal powder particles, which impact the performance of the lubricant. Therefore, this study will experimentally determine the kinematic viscosity of lubricants containing coal powder particles at different particle sizes, concentrations, and temperatures. In the experiment, the lubricant used was medium extreme pressure industrial gear lubricant N320. Coal powder was classified into three particle sizes: 0.2 mm, 0.6 mm, and 1.0 mm. The coal powder concentration was divided into three different ratios: 0.01 g/ml, 0.015 g/ml, and 0.03 g/ml. The experimental temperatures were set at 25 °C, 30 °C, 40 °C, and 50 °C. According to the orthogonal analysis method, the factors were 3, and the number of levels was 3 to 4. Based on the standard $L_{16}(4^3)$ orthogonal table for 3 factors and 4 levels, a modification was made to obtain the $L_{14}(4\times3^2)$ mixed orthogonal table. A total of 14 independent experiments were required. Additionally, the kinematic viscosity of a coal powder-free lubricant at 25 °C, 30 °C, 40 °C, and 50 °C was tested as a control group, requiring 18 independent experiments in total.

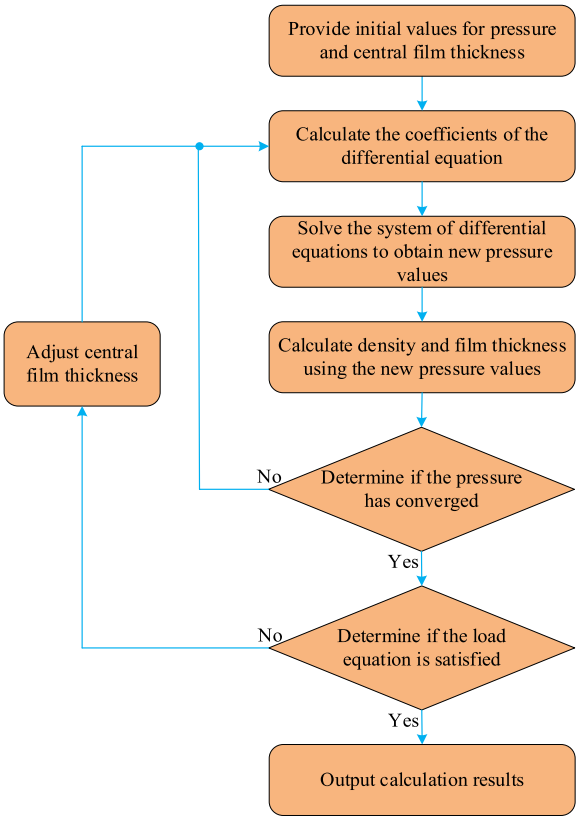

Fig. 4. Flowchart of the calculation process.

Name	N320
Density at 15 °C (kg/L)	0.903
Kinematic viscosity at 40 °C (mm^2/s)	320
Kinematic viscosity at 100 °C (mm^2/s)	25
Viscosity index	100
Flash point (open cup) (°C)	255
Pour point (not higher than) (°C)	−12

Table 3. Key technical parameters of medium extreme pressure industrial gear lubricant N320.

The specific experimental procedure is illustrated in Fig. 5. Standard sieves will be used to classify the coal powder into different particle sizes, which will then be mixed with the lubricant to prepare samples with the required particle sizes and concentrations. An ultrasonic vibrator will be employed to ensure a uniform mixture of coal powder and lubricant, after which the samples will be poured into capillary tubes. The samples will then be placed in a kinematic viscosity measuring device, heated to the specified temperature, and the kinematic viscosity will be measured using the method of measuring capillary, with the process repeated five times to obtain an average value.

The above experimental design yields data on the kinematic viscosity of coal powder-laden lubricants at different temperatures, particle sizes, and concentration ratios, as shown in Table 4.

The viscosity-temperature relationship of lubricants is typically described using the Walther equation[24], expressed as:

$$\lg\lg(v+0.7) = k - c\lg(273.15+T) \tag{11}$$

In the equation, k and c are coefficients to be determined; T represents the temperature with a unit of ℃, and ν denotes the kinematic viscosity of coal powder-laden lubricants with a unit of mm^2/s.

Based on the Walther equation, considering the effects of coal particle size and concentration on the viscosity of lubricants, and incorporating experimental data, the modified expression is:

$$\lg\lg(\nu+0.7+2.742D+155.3N+1.178D^2) = 8.588 - 3.2812\lg(273.15+T) \tag{12}$$

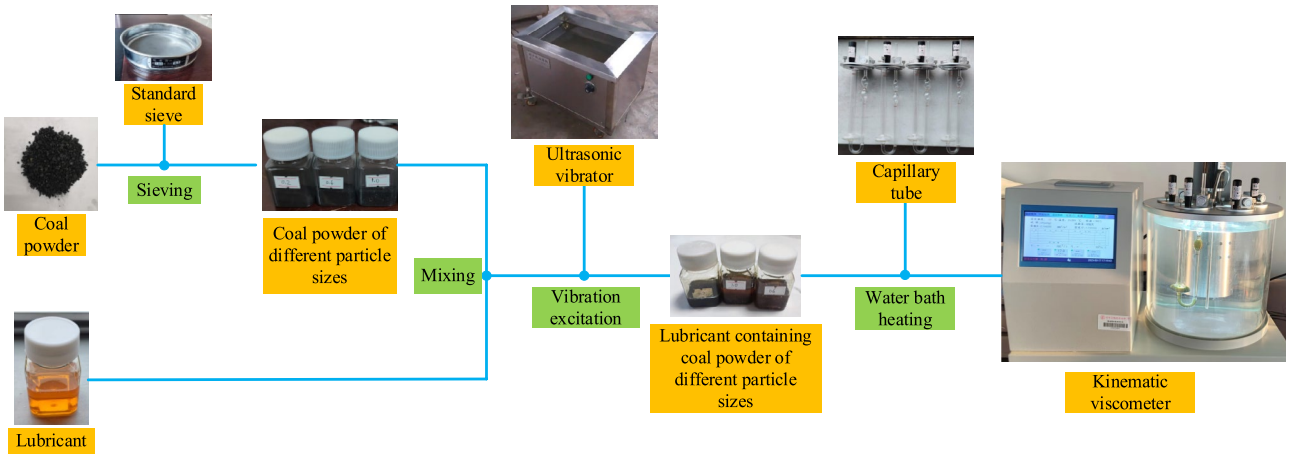

Fig. 5. Flowchart of the experiment process.

Group number	Temperature/(°C)	Coal powder particle size/(mm)	Concentration ratio/(g/ml)	Kinematic viscosity/(mm²/s)
1	25	No coal powder	-	877.59
2	25	0.2	0.01	879.63
3	25	0.6	0.015	882.25
4	25	1	0.03	886.17
5	30	No coal powder	-	612.09
6	30	0.2	0.015	615.43
7	30	0.6	0.01	615.54
8	30	1	0.03	620.66
9	40	No coal powder	-	319.74
10	40	0.2	0.03	324.92
11	40	0.6	0.03	326.23
12	40	1	0.01	324.90
13	40	1	0.015	326.35
14	50	No coal powder	-	181.35
15	50	0.2	0.03	186.53
16	50	0.6	0.03	187.83
17	50	1	0.015	187.96
18	50	1	0.01	186.50

Table 4. Values of kinematic viscosity.

The modified formula (Eq. 12) was evaluated using the R^2-statistic, yielding $R^2 = 0.982$. The R^2 value close to 1 indicates that the fitted equation aligns well with the experimental data.

Simulation analysis of gear contact characteristics in the arm transmission system

To further analyze the impact of coal powder-laden lubricants on the rocker arm drive system, a multi-software joint simulation method will be employed. The modeling process is illustrated in Fig. 6. First, a three-dimensional model of the rocker arm housing is created in Creo and imported into ANSYS in STP format, where material properties, mesh division, and constraints are set. Second the mesh of the rocker arm housing is refined using HyperMesh software to generate a.dat file. Finally, the transmission system model is established using Romax Designer software, importing the rocker arm housing.dat file, positioning the housing model, using the condense FE model command on the rocker arm housing and the transmission system components and finally completing the assembly. The cutting section of the shearer uses the YBCS-500 three-phase squirrel-cage asynchronous explosion-proof motor as the drive, with a rated power of 500 kW and a rated speed of 1470 r/min.

A driving torque of 3248 N·m is applied to the gear Z_1 shaft. Through the reduction of the rocker arm drive system, the drum operates at a speed of approximately 32 r/min during normal cutting. The drum load referenced from literature[14]. The load spectrum is shown in Fig. 7 and is applied to the model. When the shearer operates, the lubricant temperature typically exceeds 50 °C. Four operating conditions are selected: lubricant without coal powder at 50 °C, lubricant with coal powder particle size of 0.2 mm and concentration ratio of 0.01 g/ml, lubricant with coal powder particle size of 0.6 mm and concentration ratio of 0.015 g/ml, and lubricant with

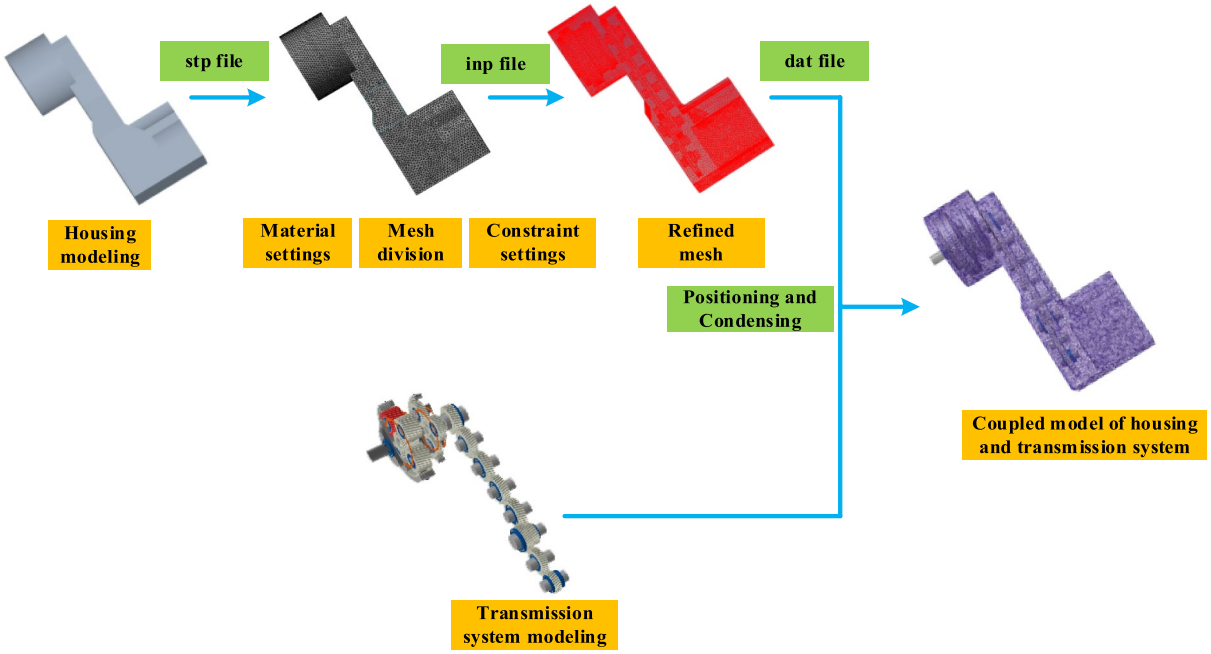

Fig. 6. Modeling process of the arm transmission system.

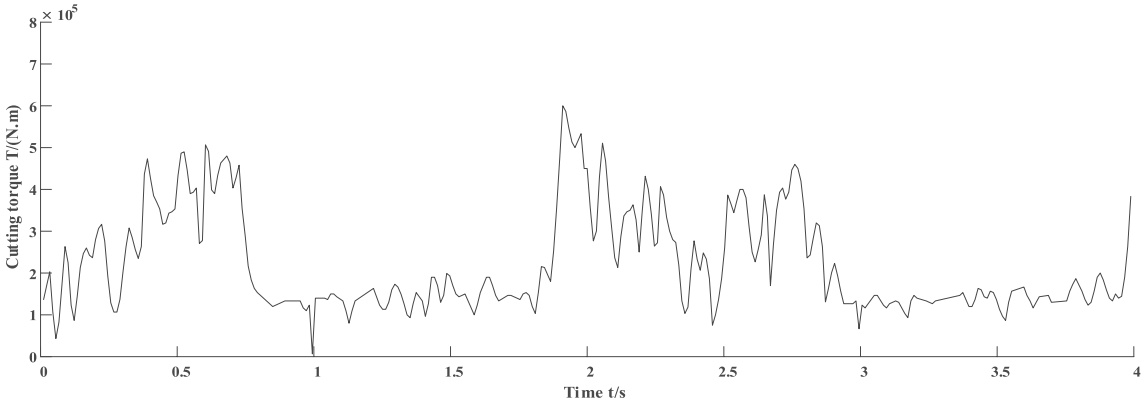

Fig. 7. Torque load spectrum of the drum.

coal powder particle size of 1 mm and concentration ratio of 0.03 g/ml. The above four operating conditions combined with the Eq. (11) to calculate the kinematic viscosity of the lubricant and input into Romax Designer for simulation analysis.

Figure 8 shows the contact stress distribution contour for a meshing cycle of the Z_1 gear under four operating conditions of above. In the case of lubricant without coal powder, the contact stress for Z_1 reaches maximum 1177 MPa. The second highest stress occurs with lubricant containing coal powder particle size of 0.2 mm and concentration ratio of 0.01 g/ml, measuring 1163 MPa. Following this, the contact stress for the condition with coal powder particle size of 0.6 mm and concentration ratio of 0.015 g/ml is 1149 MPa, while the minimum contact stress of 1134 MPa is observed with lubricant containing coal powder particle size of 1 mm and concentration ratio of 0.03 g/ml. This indicates that as the viscosity of the lubricant increases, the maximum contact stress of the gear tends to decrease. Moreover, the trends in the contact stress distribution for Z1 are generally consistent across all four conditions, with the maximum contact stress located near the input power side. In the case of the lubricant without coal powder, the maximum contact stress occurs at a tooth surface distance of 80 mm and a rolling angle of 11.188°, close to the starting point of the effective tooth profile, where the maximum value is 1177 MPa. The contact stress increases gradually from 0 to 1177 MPa within the range of tooth surface distances from 0 to 80 mm. The contact stress distribution within the range of tooth surface distances from 0 mm to 53.333 mm is relatively uniform, with contact stress gradually increasing from 0 to 757 MPa. The contact stress is relatively concentrated in two areas: The first area is between the rolling angles of 11.188° to 14.273° and tooth surface distances from 64.762 mm to 80 mm, where the contact stress increases

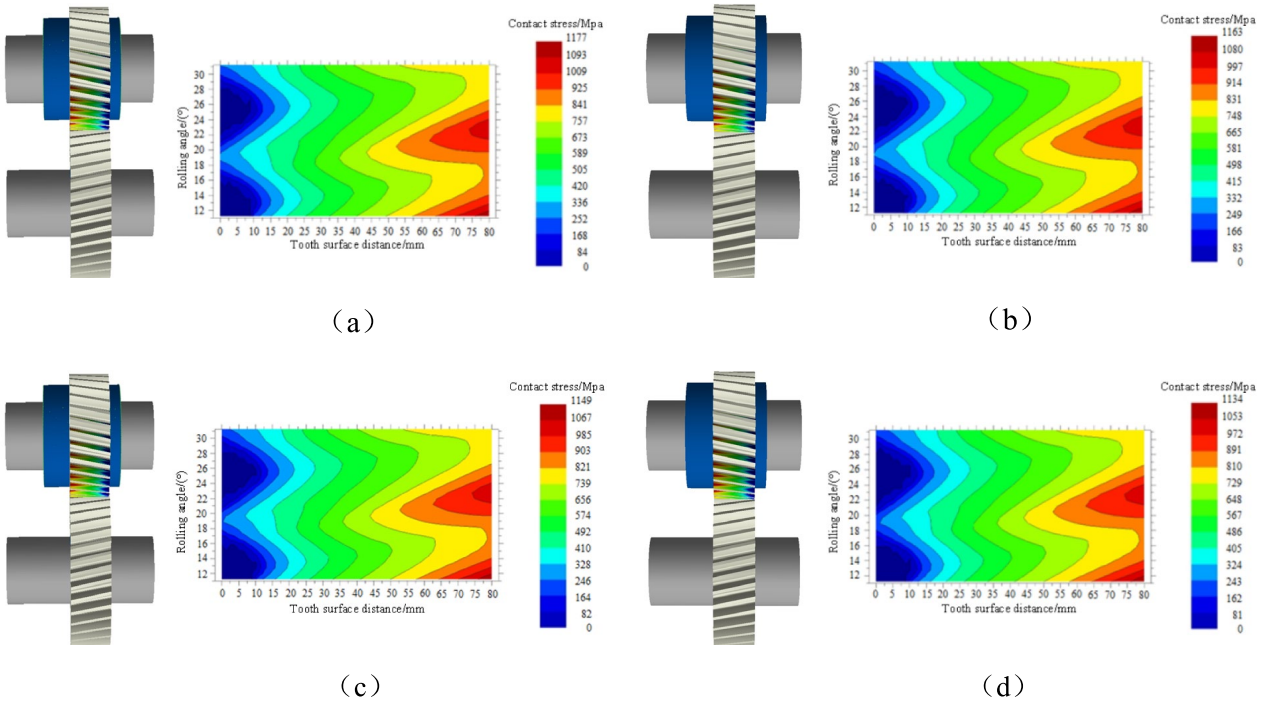

Fig. 8. Contact stress distribution contour for gear Z_1. (**a**) No coal powder. (**b**) Coal powder particle size of 0.2mm and concentration ratio of 0.01 g/ml. (**c**) Coal powder particle size of 0.6mm and concentration ratio of 0.015 g/ml. (**d**) Coal powder particle size of 1mm and concentration ratio of 0.03 g/ml.

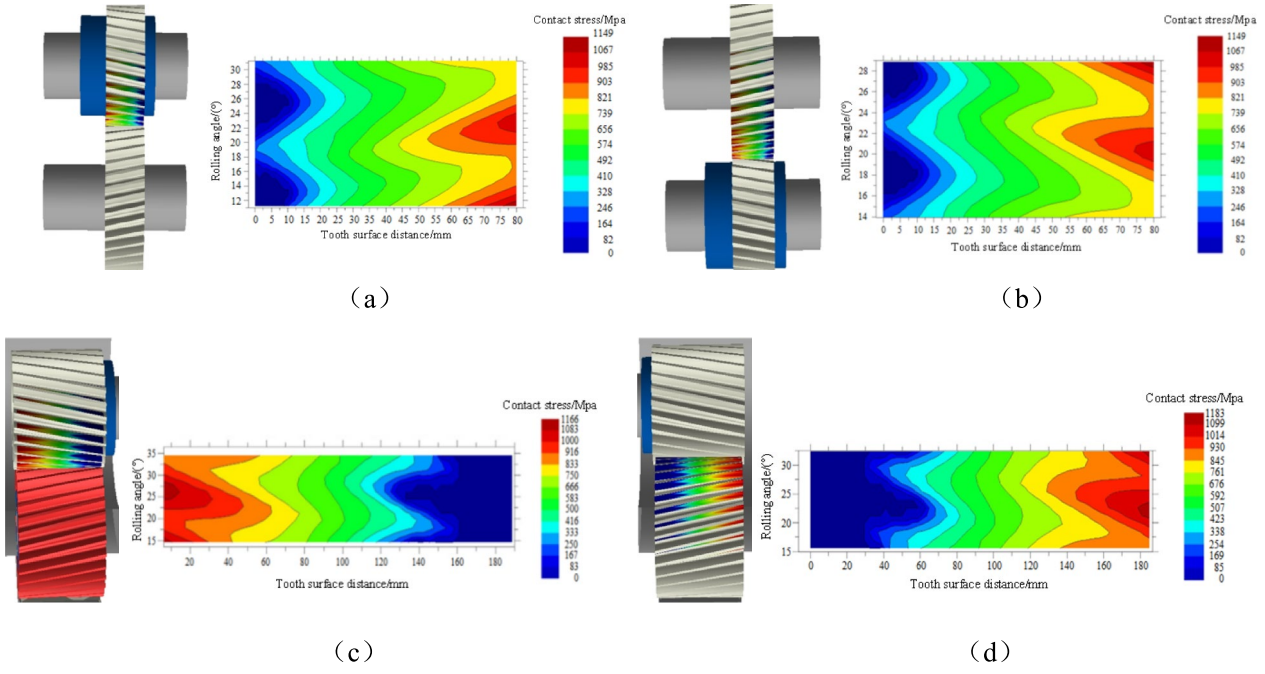

Fig. 9. Contact stress distribution contour for gears. (**a**) Gear Z_1. (**b**) Gear Z_2. (**c**) Sun gear Z_{15}. (**d**) Planet gear Z_{16}.

from 925 to 1177 MPa, forming an inverted triangle shape in the stress contour. The second area is between the rolling angles of 19.670° to 25.068° and tooth surface distances from 63.492 mm to 80 mm, where the contact stress also increases from 925 to 1177 MPa, resulting in a similar triangular shape in the stress contour.

Figure 9 shows the contact stress of different gears under the lubricant with coal powder particle size of 0.6 mm and concentration ratio of 0.015 g/ml. The maximum contact stress for gear Z_1 is 1149 MPa, for gear

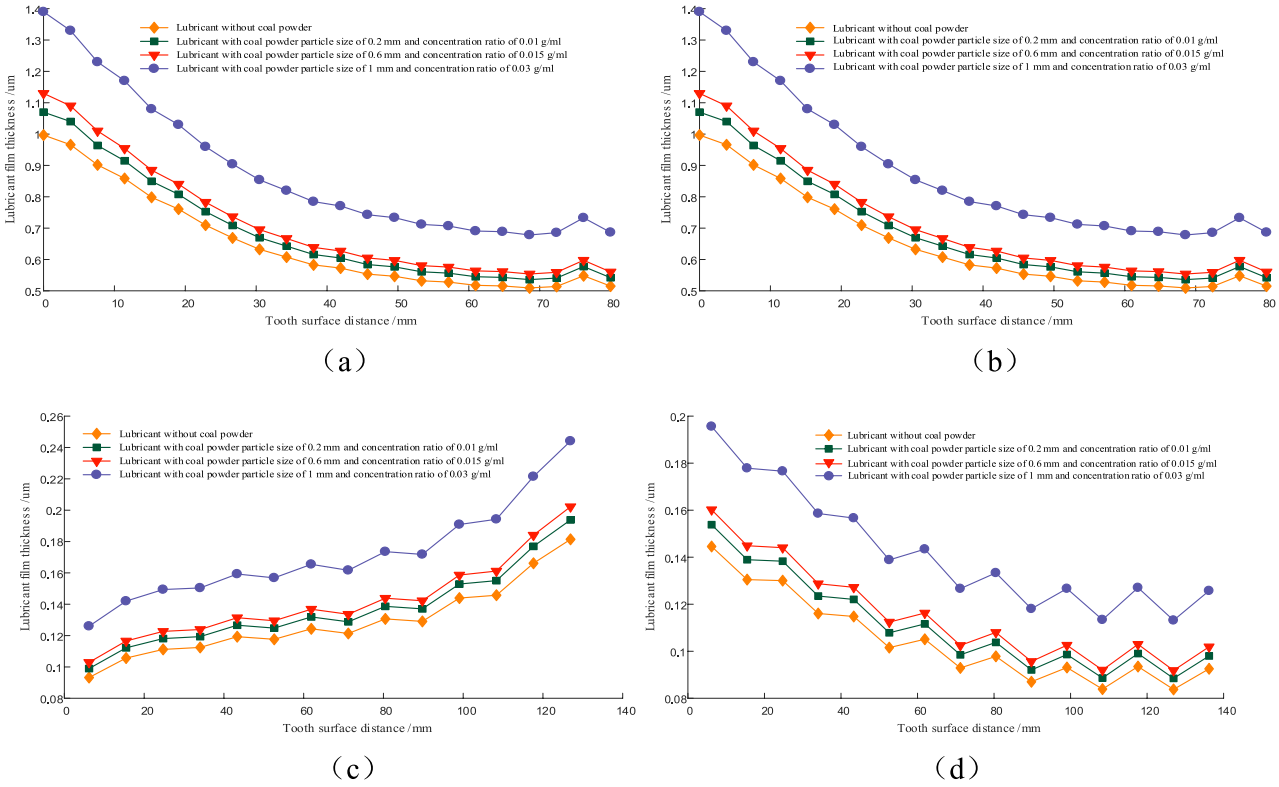

Fig. 10. Curve diagram of minimum lubricant film thickness. (**a**) Gear Z_1. (**b**) Gear Z_2. (**c**) Sun gear Z_{15}. (**d**) Planet gear Z_{16}.

Z_2 is also 1149 MPa, for sun gear Z_{15} is 1166 MPa, and for planet gear Z_{16} is 1183 MPa. It is evident that the planet gear exhibits the highest contact stress, while the contact stresses for gears Z_1 and Z_2 are relatively lower. This indicates that, after the reduction and torque increase through the rocker arm drive system, the contact stresses of the gears near the output end are significantly greater than those at the input end. The contact stress distributions for gears Z_1 and Z_2 are quite similar. In the tooth surface distance range of 20 mm to 50 mm, the contact stress distribution is relatively uniform, while it becomes concentrated in the range of 65 mm to 80 mm. For sun gear Z_{15}, the contact stress distribution is uniform in the region of 60 mm to 120 mm, with stress concentrated and relatively high in the range of 0 mm to 20 mm. The concentrated stress area for planet gear Z_{16} is located in the tooth surface distance range of 150 mm to 180 mm, with a smooth variation in strain consistent with that of sun gear Z_{15} in the range of 60 mm to 120 mm.

Figure 10 presents the minimum lubricant film thickness curve of the gear set under four operating conditions of above. The graphs for gears Z_1 and Z_2 are nearly identical, showing that the minimum lubricant film thickness decreases as the tooth surface distance increases. Furthermore, a higher concentration of coal powder in the lubricant results in an increased minimum lubricant film thickness, with a maximum value of 1.4 μm. For sun gear Z_{15}, the minimum lubricant film thickness increases in a stepped manner as the tooth surface distance increases. The higher the concentration of coal powder in the lubricant, the greater the minimum lubricant film thickness, with a maximum value of approximately 0.26 μm. In contrast, the minimum lubricant film thickness for planet gear Z_{16} decreases in a stepped manner with increasing tooth surface distance, and a higher coal powder concentration also leads to a greater minimum lubricant film thickness, with a maximum value of around 0.2 μm. Overall, the minimum lubricant film thickness without coal powder is the smallest, followed by the lubricant with coal powder particle size of 0.2 mm and concentration ratio of 0.01 g/ml, then the lubricant with particle size of 0.6 mm and concentration ratio of 0.015 g/ml, while the lubricant with particle size of 1 mm and concentration ratio of 0.03 g/ml has the greatest lubricant film thickness. This indicates that the viscosity of the lubricant and the concentration of coal powder are positively correlated with the minimum lubricant film thickness.

Conclusions

To study the contact characteristics of the arm gear transmission system of shearer under lubrication containing coal powder impurities, a multi-software collaborative simulation method was employed to construct a simulation model of the arm gear transmission system. The effects of different coal powder particle sizes and concentrations of the lubricant containing coal powder on the contact stress and lubricant film thickness of the gear set were analyzed, leading to the following conclusions:

(1) For lubricants containing coal powder, the particle size and concentration of coal powder significantly affect the viscosity of the lubricant. At a constant temperature, the viscosity of the lubricant increases with the particle size and concentration of coal powder.

(2) The maximum contact stress of the gear set in the arm transmission system decreases with increasing coal powder particle size and concentration. Under the same lubricant viscosity conditions, the contact stress of the gears near the output end is significantly greater than that of the input end.

(3)The minimum lubricant film thickness between the gears of the arm transmission system decreases with increasing tooth surface distance, and it is positively correlated with the particle size and concentration of coal powder in the lubricant; the larger the particle size and concentration, the greater the lubricant minimum film thickness.

Data availability

All data generated or analysed during this study are included in this published article.

Received: 10 January 2025; Accepted: 25 August 2025
Published online: 26 September 2025

References

1. Lü, Z. H. Analysis of contact stress characteristics of gear pair based on hertz theory. *J. Lanzhou lnst. Technol.* **30**(03), 5–8 (2023).
2. Wang, Y. D. et al. Calculation and analysis of meshing contact of lnvolute spur gear. *J. Mech. Transm.* **45**(12), 41–47 (2021).
3. Feng, J. J., Jian, Z. H. & Chen, H. Analyses of contact stresses in transmission process of lnvolute spur cylindrical modified gear. *Mach. Tool Hydraul.* **51**(20), 106–111 (2023).
4. Xiang, L., Fang, Z. D., Guan, Y. B. & Hu, S. Y. A hybrid analytical method for calculating contact stress of helical gear with assembly error. *J. Harbin Eng. Univ.* **40**(10), 1767–1775 (2019).
5. Li, G. Y. & Zhou, D. R. Simulation analysis of dynamic contact process of spur gear meshing. *J. Lanzhou Univ. Technol.* **38**(04), 27–30 (2012).
6. Yang, S. Study on Accurate Calculation of the Contact Stress of lnvolute Spur Gears. 2016(02):17–20.
7. Liu, G. H., Wang, Q. & Tang, N. F. Fatigue life analysis of the plastic helical gear and steel worm transmission mechanism. *J. Mech. Transm.* **47**(01), 126–131 (2023).
8. Fan, Z. M., Zhang, X. W. & Ma, Y. D. Contact stress of double involute gear based on fractal theory. *Tribology* **39**(02), 150–156 (2019).
9. Huang, X. M. Numerical analysis method and test for contact stress of cycloidal gear in RV reducer. *China Mech. Eng.* **34**(24), 3015–3023 (2023).
10. Frankovský, P., Ostertag, O., Trebuňa, F., Ostertagová, E. & Kelemen, M. Methodology of contact stress analysis of gearwheel by means of experimental photoelasticity. *Appl. Optics* **55**(18), 4856–4864 (2016).
11. Yang, X. P. et al. Numerical and experimental research of helical gear contact stress considering the influence of friction. *Front. Mech. Eng.* **8**, 1078134 (2022).
12. Wang, S. H., Hu, B., Wu, Z. Y., Zhou, Y. S. & Tang, J. Y. A comprehensive optimization model of tooth surface parameters for the minimization of contact stress of helical face gears by considering the avoidance of edge contact. *Mathematics* **10**(17), 3102 (2022).
13. Chen, L., Hao, C. J., Wang, Z. H., Feng, W. B. & Yang, Y. M. Isogeometric analysis of gear with single tooth contact. *J. Mech. Eng.* **57**(03), 107–115 (2021).
14. Mao, J., Zhu, Y., Chen, H. Y., Yuan, Z. & Song, Z. D. Life prediction and optimization analysis of shearer rocker arm's transmission system. *J. Mach. Des.* **35**(12), 52–58 (2018).
15. Cui, H.B. Contact Stress Simulation Analysis of lnvolute Cylindrical Spur Gear Based on MATLAB and SolidWorks Joint Modeling. lnternal Combustion Engine & Parts, 2022(04):63–66.
16. Liu, A. M., Han, Y. Z. & Wang, L. H. The finite element analysis of contact stress for helical gear transmission during meshing process. *Mach. Des. Res.* **29**(03), 35–38 (2013).
17. Yang, F., Fu, Z. Y. & Tian, Z. D. Simulation analysis of gear contact stress in reduction gearbox. *J. Phys.: Conf. Ser.* **1748**(6), 062072 (2021).
18. Yan, G. P., Yu, D. H. & Zhong, F. Dynamic contact stress analysis of spur gear modification based on modification condition. *Mach. Des. Manuf.* **08**, 193–196 (2022).
19. Wei, Y. G. & Guan, R. R. FEA of contact stresses in lnvolute cylindrical gear meshing. *J. Dalian Jiaotong Univ.* **30**(02), 22–25 (2009).
20. Zhao, G. F., Guo, Y. C. & Liu, D. W. Contact-stress analysis in meshing process of involute cylindrical spur gear. *Mach. Des. Manuf.* **03**, 52–54 (2008).
21. Li, J., Li, H. C., Wang, W. C., Li, K. K. & Guo, D. N. Strength check and stress simulation for the gear of a high-pressure aero-fuel gear pump. *Chinese Hydraul. Pneum.* **02**, 105–113 (2021).
22. Pu, L. G., Chen, G. D. & Wu, L. Y. *Mechanical Design* 10th edn. (Higher Education Press, 2019).
23. Wen, S. Z. & Yang, P. R. *Elastic Fluid Film Lubrication* (Tsinghua University Press, 1992).
24. Walther, C. The evaluation of viscosity data. *Erdol Teer* **7**(2), 382–384 (1931).

Acknowledgements

This work was supported in part by the National Natural Science Foundation of China under Grant 52004119, in part by the Liaoning Provincial Department of Education under Grant LJ212410147024, in part by the GPU resource pool support project of Liaoning Technical University under Grant 2024-14, in part by the National Natural Science Foundation of China under Grant 52204215, in part by the Liaoning Provincial Natural Science Foundation Joint Fund Project under Grant 20240325. And our deepest gratitude goes to the anonymous reviewers for their careful work and thoughtful suggestions that have helped improve this paper substantially.

Author contributions

Xin Wang: Conceptualization, Methodology; Rennan Wu: Writing—Original Draft, Data curation,Software; Libin Wang: Investigation， Validation; Yangxi Bai: Resources; All authors reviewed the manuscript.

Funding
National Natural Science Foundation of China,52004119,Liaoning Provincial Department of Education,LJ212410147024,GPU resource pool support project of Liaoning Technical University,2024-14,the National Natural Science Foundation of China,52204215,the Liaoning Provincial Natural Science Foundation Joint Fund Project,20240325

Declarations

Competing interests
The authors declare no competing interests.

Additional information
Correspondence and requests for materials should be addressed to R.W.

Reprints and permissions information is available at www.nature.com/reprints.

Publisher's note Springer Nature remains neutral with regard to jurisdictional claims in published maps and institutional affiliations.